



# The dynamical evolution of accreted star clusters in the Milky Way

M. Miholics, J. J. Webb, and A. Sills

Department of Physics & Astronomy, McMaster University, 1280 Main St. W., Hamilton, Ontario, L8S 4L8, Canada, e-mail: miholim@mcmaster.ca

**Abstract.** We perform  $N$ -body simulations of star clusters in time-dependant galactic potentials. Since the Milky Way (MW) was built-up through mergers with dwarf galaxies, its globular cluster population is made up of clusters formed both during the initial collapse of the Galaxy and in dwarf galaxies that were later accreted. Throughout a dwarf-MW merger, dwarf galaxy clusters are subject to a changing galactic potential. Building on our previous work, we investigate how this changing galactic potential affects the evolution of a cluster's half mass radius. In particular, we simulate clusters on circular orbits around a dwarf galaxy that either falls into the MW or evaporates as it orbits the MW. We find that the dynamical evolution of a star cluster is determined by whichever galaxy has the strongest tidal field at the position of the cluster. Thus, clusters entering the MW undergo changes in size as the MW tidal field becomes stronger and that of the dwarf diminishes. We find that ultimately accreted clusters quickly become the same size as a cluster born in the MW on the same orbit. Assuming their initial sizes are similar, clusters born in the Galaxy and those that are accreted cannot be separated based on their current size alone.

## 1. Introduction

Almost all types of galaxies in our Universe are known to host a population of globular clusters (GCs). Since galaxies are formed through hierarchal merging (White & Rees 1978), the GC population of any given galaxy is comprised of GCs formed in its smaller constituent galaxies (Searle & Zinn 1978). Many examples of GC accretion exist in the present day Universe, including approximately 5 GCs being accreted onto the MW with the Sagittarius dwarf galaxy (e.g. Da Costa & Armandroff 1995; Palma et al. 2002; Bellazzini et al. 2003; Law & Majewski 2010). Consequently, GCs are an excellent means for tracing some aspects of their host galaxy's evolution. For example, properties such as age, metallicity and horizon-

tal branch morphology have been used to estimate what fraction of the MW GCs have been accreted and subsequently estimate how many dwarf galaxies have merged with the MW in the past (e.g Mackey & Gilmore 2004; Marín-Franch et al. 2009; Forbes & Bridges 2010; Leaman et al. 2013).

Since the dynamics of GCs can be significantly affected by the tidal field of their host galaxy (e.g. Baumgardt & Makino 2003; Webb et al. 2014a,b), it may be possible to also use the structural properties of GCs, such as mass and size, to identify accreted clusters from in situ. To apply this idea, we must first know how the dynamical evolution and subsequently the observed properties of GCs are effected by the merging process. The aim of the work presented here is to quantify the ef-

fect of the changing gravitational potential of a galaxy merger on the dynamics of accreted clusters. This work was done in the specific context of a cluster born in a dwarf galaxy being accreted onto the MW, however, the results may be applied to any cluster experiencing a changing tidal field. Please note the results presented here have been published previously in the Monthly Notices of the Royal Astronomical Society as Miholics et al. (2016). Some excerpts of that work are included in the text here.

## 2. Methods

To simulate clusters in time dependent tidal fields, we utilize the code NBODY6TT (Renaud et al. 2011; Renaud & Gieles 2015), an extension of NBODY6 (Aarseth 1999, 2003; Nitadori & Aarseth 2012) designed to evolve star clusters in arbitrary time dependant galactic potentials. The use of NBODY6TT requires the user to specify a time series of tidal tensors which the code uses to calculate the tidal forces on the cluster stars. This method allows the user to completely specify the time and space variation of the galactic potential as well as the orbit of the cluster in the potential.

In a dwarf-MW merger there are two key processes that will affect the evolution of a star cluster. The first relevant process is the increase of the MW tidal field strength on the cluster as the dwarf falls closer to the centre of the MW. The second process is the decrease in the dwarf’s tidal field strength as the MW strips material away from the dwarf and the dwarf becomes less massive. We study the effect of each of these processes separately by simulating clusters in two different scenarios, which we will call “dwarf falls” and “dwarf evaporates”, described in the next section. In this contribution, we present one simulation in each of the scenarios using our fiducial cluster and galaxy parameters. The cluster is initialized with 50,000 stars in a Plummer density profile (Plummer 1911) with a half mass radius,  $r_m = 3.2$  pc. The initial stellar masses are assigned using a Kroupa (2001) IMF and velocities are assigned such that cluster is initially virialized. For more information about

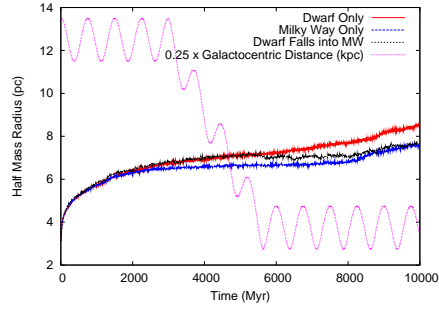


**Fig. 1.** Half mass radius for the cluster in three potentials: dwarf only (red) at 4 kpc, MW at 15 kpc only (blue) and in the combined potential of the dwarf falling into the MW (black). The magenta line gives 0.25 x the distance between the cluster and the MW in kpc.

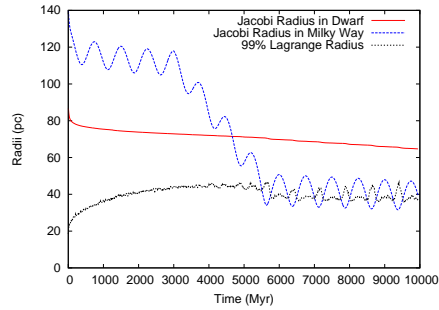


**Fig. 2.** The Jacobi radius of the cluster in the dwarf (red) and in the MW (blue) as defined by Equation 1. We also plot the cluster’s 99 per cent Lagrange radius,  $r_{99}$  in black.

the method and the full suite of simulations, please refer to Miholics et al. (2016).

## 3. Results

### 3.1. Dwarf falls into MW

In our first simulation, we evolve the cluster on a circular orbit around a point mass dwarf ( $M_D = 10^9 M_\odot$  and  $R = 4.0$  kpc) which is located 50 kpc from the centre of the MW (represented by a bulge+disk+halo potential). After 3 Gyr, we allow the distance between the dwarf and MW to decrease until the separation between the two galaxies is 15 kpc. In Figure 1, we plot the half mass radius for a cluster in

such a potential. For comparison, we also show clusters in the dwarf only and in the MW only (orbiting on a circular orbit of  $R = 15$  kpc).

We can understand the cluster's size evolution in the combined potential by considering Figure 2, where we plot the Jacobi radius of the cluster in each of the individual galaxies as a function of time. The Jacobi radius is calculated in each galaxy using the following:

$$r_j = R_G \left( \frac{M_c}{3M_G} \right)^{1/3} \quad (1)$$

where  $R_G$  is the radius of the circular orbit,  $M_c$  is the cluster's mass and  $M_G$  is the mass of the galaxy enclosed by the cluster's orbit (von Hoerner 1957). From this point in the text, the two values of Jacobi radius in the dwarf and Jacobi radius in the MW will be abbreviated as  $r_j^D$  and  $r_j^{MW}$  respectively.

The evolution of the cluster's half mass radius in the combined potential is almost identical to its evolution in only the dwarf galaxy over the first several Gyr of the cluster's lifetime. This similarity indicates that when the dwarf is far from the MW centre, the dwarf tides dominate the cluster. This idea is reinforced by Figure 2 which shows that  $r_j^D$  is much smaller than  $r_j^{MW}$  during the first stage of the cluster's life. However, as the dwarf falls into the MW, the  $r_j^{MW}$  shrinks (the tides become stronger) and the MW becomes the dominant galaxy in terms of tidal field strength. At about 5.5 Gyr (2.5 Gyr after the dwarf starts to fall into the MW) the cluster's half mass radius suddenly starts to decrease. By examining Figure 2, we see that this sudden decrease corresponds to the time when  $r_j^{MW}$  has decreased to a value such that  $r_{99}$  (the cluster's 99% Lagrange radius) becomes roughly equal to it. At this point, the cluster completely fills its Jacobi radius in the MW and becomes very susceptible to tidal stripping. A short time after the dwarf reaches its final position in the MW, at a separation of 15 kpc, the cluster's half mass radius completely overlaps with the half mass radius of the cluster that has evolved in the MW only.

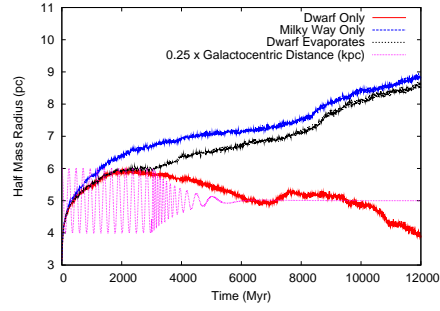


**Fig. 3.** Half mass radius over time in the three potentials as well as  $0.25 \times$  the Galactocentric distance in the MW. Colours are the same as in Figure 1.

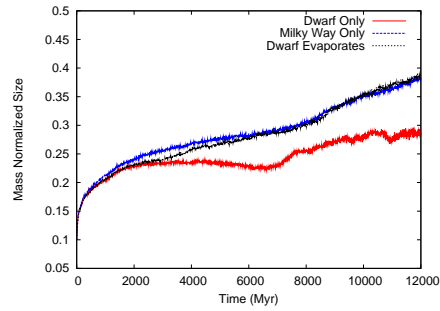


**Fig. 4.** Mass normalized size ( $r_m/M^{(1/3)}$ ) of the cluster over time in the three potentials: dwarf only (red), MW (blue), combined potential (black).

### 3.2. Dwarf evaporates

In our second scenario, we evolve a cluster on a circular orbit around a point mass dwarf galaxy ( $M_D = 10^{10} M_\odot$ ,  $R = 4.0$  kpc) that in turn executes a circular orbit ( $R = 20.0$  kpc) around the centre of the MW. After 3 Gyr of evolution in this system, we decrease the mass of the dwarf and radius of the cluster's orbit in the dwarf smoothly to zero, eventually leaving the cluster on a circular orbit in the MW at 20.0 kpc.

In Figure 4, we show the cluster's half mass radius over time in this potential. Initially, the cluster follows an evolution similar to its evolution in the dwarf galaxy only, showing that the dwarf's tides dominate over the MW tides in this configuration. When the mass of the dwarf begins to decrease, the tides weaken and we see an immediate increase in the cluster's half mass radius. By 6 Gyr, the dwarf's mass

is effectively zero and the cluster is orbiting in the MW only. The half mass radius of the cluster continues to expand and becomes very close to the half mass radius of the cluster living in the MW its whole life. To remove the effect of varying mass loss rates in different potentials, in Figure 4, we have shown the mass normalized radius ( $r_m/M^{1/3}$ ) in the three potentials. After the dwarf evaporates, we see that mass normalized radius overlaps completely with the mass normalized radius for the cluster in the MW potential only. Hence, the remaining difference in the clusters' half mass radii in these two potentials can be attributed to differences in cluster mass. For further discussion of the effect of varying mass loss rates on the cluster size, see Miholics et al. (2016).

#### 4. Summary

Taking all the results from the above simulations together, we can construct the full picture of a star cluster's evolution inside a dwarf-MW merger. The two scenarios used represent the key processes affecting a cluster in this type of galaxy merger. These processes have the same net effect, to increase the MW's tidal field with respect to that of the dwarf. The simulations we performed show that a cluster will have a size determined by whichever tidal field is the strongest at any one point. Whenever the MW's tides take over, the cluster will respond quickly to the new potential and ultimately become the same size as a cluster that has evolved solely in the MW. Thus, the main conclusions of this work are that it should be impossible to distinguish between clusters born inside and outside the MW based on size alone and the distributions of tidally filling and underfilling clusters in the MW should not be affected by the presence of clusters accreted from dwarf galaxies (assuming initial cluster sizes for accreted and in situ clusters are the same).

*Acknowledgements.* We thank Florent Renaud for his assistance with NBODY6TT and the referee of

the original work for constructive comments. We acknowledge the use of SHARCnet resources. M.M., A.S. and J.W. were supported by NSERC during the completion of this work.

#### References

- Aarseth, S. J. 1999, *PASP*, 111, 1333  
Aarseth, S. J. 2003, *Gravitational N-Body Simulations* (Cambridge University Press, Cambridge)  
Baumgardt, H. & Makino, J. 2003, *MNRAS*, 340, 227  
Bellazzini, M., Ferraro, F. R., & Ibata, R. 2003, *AJ*, 125, 188  
Da Costa, G. S. & Armandroff, T. E. 1995, *AJ*, 109, 2533  
Forbes, D. A. & Bridges, T. 2010, *MNRAS*, 404, 1203  
Kroupa, P. 2001, *MNRAS*, 322, 231  
Law, D. R. & Majewski, S. R. 2010, *ApJ*, 718, 1128  
Leaman, R., VandenBerg, D. A., & Mendel, J. T. 2013, *MNRAS*, 436, 122  
Mackey, A. D. & Gilmore, G. F. 2004, *MNRAS*, 355, 504  
Marín-Franch, A., Aparicio, A., Piotto, G., et al. 2009, *ApJ*, 694, 1498  
Miholics, M., Webb, J. J., & Sills, A. 2016, *MNRAS*, 456, 240  
Nitadori, K. & Aarseth, S. J. 2012, *MNRAS*, 424, 545  
Palma, C., Majewski, S. R., & Johnston, K. V. 2002, *ApJ*, 564, 736  
Plummer, H. C. 1911, *MNRAS*, 71, 460  
Renaud, F. & Gieles, M. 2015, *MNRAS*, 448, 3416  
Renaud, F., Gieles, M., & Boily, C. M. 2011, *MNRAS*, 418, 759  
Searle, L. & Zinn, R. 1978, *ApJ*, 225, 357  
von Hoerner, S. 1957, *ApJ*, 125, 451  
Webb, J. J., et al. 2014a, *MNRAS*, 442, 1569  
Webb, J. J., et al. 2014b, *MNRAS*, 445, 1048  
White, S. D. M. & Rees, M. J. 1978, *MNRAS*, 183, 341